Confocal Raman Studies of the Evolution of the Physical State of Mixed Phthalic Acid/Ammonium Sulfate Aerosol Droplets and the Effect of Substrates

ARTICLE *in* THE JOURNAL OF PHYSICAL CHEMISTRY B · MAY 2014

Impact Factor: 3.3 · DOI: 10.1021/jp5004598 · Source: PubMed

5 AUTHORS, INCLUDING:

Zhou Qiang
Chinese Academy of Sciences
3 PUBLICATIONS **14** CITATIONS

SEE PROFILE

THE JOURNAL OF PHYSICAL CHEMISTRY B

Article

pubs.acs.org/JPCB

Confocal Raman Studies of the Evolution of the Physical State of Mixed Phthalic Acid/Ammonium Sulfate Aerosol Droplets and the Effect of Substrates

Qiang Zhou, Shu-Feng Pang, Yang Wang, Jia-Bi Ma,* and Yun-Hong Zhang*

The Institute of Chemical Physics, Key Laboratory of Cluster Science, School of Chemistry, Beijing Institute of Technology, Beijing 100081, People's Republic of China

Supporting Information

ABSTRACT: The confocal Raman spectra of mixed phthalic acid/ammonium sulfate (AS) droplets deposited on a polytetrafluoroethylene (PTFE) substrate and a hydrophilic glass substrate are collected. The evolution of the physical state of the mixed droplet deposited on the PTFE substrate at various relative humidities consists of three states: well-mixed liquid state, liquid–liquid phase-separated state, and crystalline state. When the mixed droplets exist in liquid–liquid phase-separated state, the morphologies of the droplets on a PTFE substrate and on a glass slide are totally reverse, that is, an aqueous AS inner phase surrounded by an organic outer phase and an organic inner phase surrounded by an AS outer phase, respectively. We propose that the salting-out effect may induce the diffusion and formation of the organic phase, thus leading to the generation of liquid–liquid phase separation. The surface tension and hydrophobicity/hydrophilicity of substrates influence the spatial distribution of mixed aerosols. The understanding about the evolution of the physical state of mixed droplets and the effect of the substrates are important for probing the formation of atmospheric aerosols' morphology in the dehumidifying process.

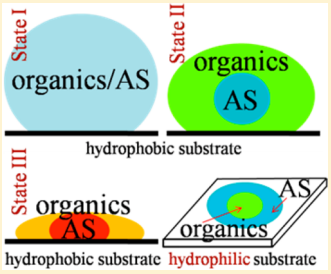

1. INTRODUCTION

In the atmosphere, single particles containing both organic and sulfate species are abundant.[1,2] Because the sulfate fraction is often partially or fully neutralized by ammonium, mixed organic/ammonium sulfate (AS) particles constitute an important class of atmospheric aerosol particles.[3,4] Their characterization is instructive to elucidate the influence of aerosols on visibility, climate, and human health.[5−7] In detail, organic and inorganic particles have a direct impact on earth's radiation balance and climate due to light absorbing and scattering. For example, particles composed of elemental carbon (EC) absorb light and have a warming effect on the climate.[8] In contrast, particles composed of sulfate (SO_4^{2-}) scatter light rather than absorb it and thus have a cooling effect on climate.[9] Meanwhile, they indirectly act as cloud condensation and ice nuclei, modifying cloud properties. Several essential ingredients inducing the aerosol size, physical state, chemical composition, and morphology influence these effects previously mentioned.[7,10] Therefore, the interrelation between chemical composition and aerosol phase state is critical to attain correct descriptions of aerosol effects on climate.

The inorganic aerosol constituents are relatively small in number and well-known. However, the chemical composition of the organics is highly complex and still far from clear.[11,12] Field measurements showed that organic aerosol accounts for 30 to 80% of the total fine aerosol mass in various regions.[13,14]

Although the investigations about mixed organic/inorganic aerosol particles draw increasing attention, the physical state of these systems is not well characterized.[15] The physical state of aerosol particles depends on the chemical composition, relative humidity (RH), and temperature.[16−19] Because of these factors, atmospheric aerosol particles may present as different states, for example, one liquid phase, two liquid phases, crystalline phases, a glassy state, or mixture of these phases.[19] RH is a crucial factor for aerosol particles. Aerosol particles will undergo phase transitions when exposed to varying humidities in the atmosphere, such as, efflorescence, deliquescence, and liquid–liquid phase separation (LLPS) (two liquid phases). Particles in liquid–liquid phase-separated state can adopt core–shell structures or asymmetric partial engulfed structures. Obtaining the knowledge of the aerosol morphology through investigating the influences of RH is indispensable for determining the nature of the gas-particle interface and the rates of heterogeneous chemical reactions as well as the kinetics of water uptake.[16,17]

A large amount of literature is now available on LLPS. Ciobanu et al. used optical microscopy and micro-Raman spectroscopy to investigate LLPS of micrometer-sized droplets consisting of poly(ethylene glycol)-400 (PEG-400)/AS/water, and the resulting morphology was an aqueous AS inner phase surrounded by a mainly PEG-400 containing outer phase.[15] The liquid–liquid phase-separated mechanisms are also identified for the PEG-400/AS/H_2O system.[15] Song et al. measured Mie spectra of PEG-400/AS/water at ∼93.5% and at ∼80.9% RH, and the results were in good agreement with the

Received: January 15, 2014
Revised: May 19, 2014
Published: May 19, 2014

   dx.doi.org/10.1021/jp5004598 | J. Phys. Chem. B 2014, 118, 6198−6205

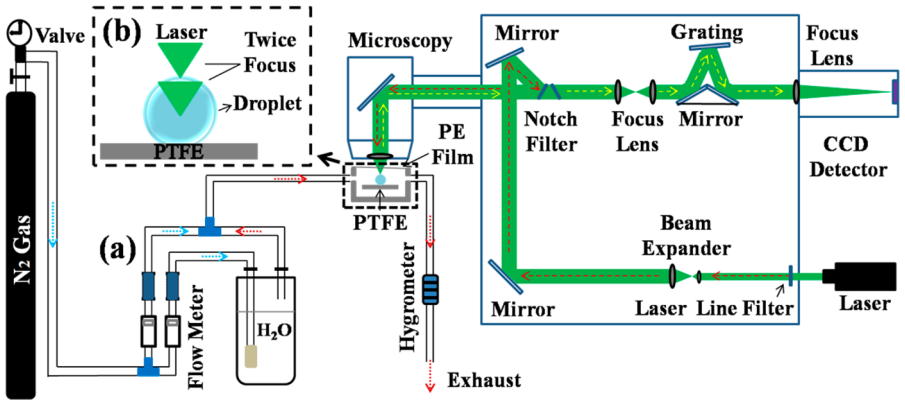

Figure 1. (a) Schematic diagram of the experimental setup for the ambient RH adjustment and the confocal Raman measurements. (b) Twice focused laser on a mixed droplet deposited on a PTFE substrate.

computed Mie spectra for a homogeneous and a core−shell configuration, respectively. The authors suggest that the core−shell morphology is the prevalent configuration of liquid−liquid phase-separated tropospheric organic/AS/water particles.[20] What's more, Bertram and coworkers observed core−shell morphologies in mixed organic/AS particles deposited on a hydrophobically coated substrate.[21] You et al. investigated 23 organics mixed with four different salts, a total of 92 different particle types, and reported that out of the 92 types, 49 underwent LLPS.[22] Song et al. also pointed out that for atmospheric relevant mixtures consisting of organics/AS/water with up to 10 organic components, LLPS always occurred for oxygen-to-carbon atomic ratios (O:C) < 0.56 and depended on the specific types of organic functional groups in the range of 0.56 < O:C < 0.80.[23] Furthermore, Ciobanu and coworkers reported that the kinetics of phase separation depend on particle size, the ratio of PEG-400/AS, surface tension effects, and diffusion of AS ions and inclusions.[15]

It is noteworthy that the evolution of the physical state of the ambient aerosols in a dehumidifying process has not yet been experimentally detected. In addition, how to describe the evolution of the physical state in the dehumidifying process and the substrate effects by means of spectrometer is an interesting question. The present study aims at exploring efflorescence of AS in mixed organic/AS/water particles and the evolution of the physical state as well as the effect of substrates by employing confocal Raman spectroscopy in conjunction with optical microscopy.

We choose mixed phthalic acid/AS droplets on a polytetrafluoroethylene (PTFE) and a hydrophilic glass slide substrates as the model system. Phthalic acid ($C_8H_6O_4$) is a dicarboxylic acid with O:C = 0.5, which is in the O:C ranges of LLPS specified by Song et al.,[23] and it is also an important industrial material used for plastic production[24] such as polyester fiber and polyethyleneterephthalate (PET) thermoplastics. It can be directly produced by burning plastic wastes and is ubiquitous in the atmosphere.[25,26] Concerning the inorganic component, AS is chosen due to its broad existence in the atmosphere and its well-characterized thermodynamic and spectroscopic properties.[27−31]

2. EXPERIMENTAL SECTION

2.1. Sample Preparation. A stock solution of mixture with organic-to-inorganic molar ratios (OIRs) = 1:3 (c_{AS} = 1.5 mol/L) and 1:6 (c_{AS} = 3 mol/L) is prepared by dissolving analytical-grade phthalic acid (S = 0.413 g/100 g water)[32] and AS (S = 75.372 g/100 g water)[33] in deionized water without further purification. Phthalic acid is in solid state at room temperature. By using a syringe, droplets of the solution are injected and sprayed onto a PTFE substrate fixed to the bottom of the chamber. It is reported that a water droplet on PTFE has a contact angle of ∼133.5°.[34] The effect of gravity on the micro droplets can be neglected,[35] and thus mixed phthalic acid/AS droplets on the PTFE film have little interface with the substrate, and the shape of the droplets is nearly spherical, in resemblance to that of airborne atmospheric aerosols. The contact angle of phthalic acid droplet on the PTFE film is ∼126.43°, as shown in Figure S1 (see the Supporting Information), and the contact angles of mixed phthalic acid/AS droplets on the PTFE film are ∼133.07 (OIR = 1:3) and ∼135.59° (OIR =1:6).

When liquid−liquid phase-separated process occurs, the two liquid phases should have different composition distributions. To describe the composition difference between the center and the surface regions of the mixed droplet, we calculated the peak area ratio R of the $\nu_s(SO_4^{2-})$ band of AS to the ν(C═C) and ν(C═O) bands of phthalic acid by using the following formulas

$$R = A_{980}/(A_{1590} + A_{1600} + A_{1640} + A_{1709}) \quad (1)$$

$$\Delta R = R_{center} - R_{surface} \quad (2)$$

where A and the subscripts denote the peak areas and the corresponding band positions, respectively.

Then, the chamber is sealed with a piece of transparent polyethylene (PE) film. The RH in the chamber can be precisely controlled by the mass flow meter (Alicat scientific) to mix and adjust two flows of dry and water-saturated nitrogen gas. The real-time RH can be monitored by the humidity temperature meter (Centertek Center 310) with an accuracy of ±2.5% RH and ±0.7 °C. After being stabilized for ∼0.5 h at a given RH in the chamber, the confocal Raman measurement is made for droplets in diameters from 30 to 100 μm, as observed through a 50× objective of the Leica DMLM microscope.

2.2. Confocal Raman Measurements. A schematic diagram of the experimental apparatus is shown in Figure 1a. It consists of two mainly functional parts, that is, a chamber for adjusting the ambient RH of mixed droplets and a confocal Raman system (Ranishaw inVia) for measuring Raman spectra and imaging morphological changes of mixed droplets. A 514.5 nm argon-ion laser with an output power of 20 mW is used as

dx.doi.org/10.1021/jp5004598 | J. Phys. Chem. B 2014, 118, 6198−6205

the excitation source. Before the Raman measurement of the droplets, a calibration is made with respect to the 520 cm^{-1} silicon band. A 514.5 nm notch filter is used to remove the strong Rayleigh scattering. The backscattering signals passing through a 1800 g/mm grating of the monochromator are subsequently detected and recorded by a charge-coupled device (CCD). The Raman spectra from 400 to 4000 cm^{-1} with 1 cm^{-1} resolution are obtained with three repeated scans, and each scan has an exposure time of 10 s. All measurements are made at ambient temperatures of 22−24 °C with a spectral reproducibility of 0.2 cm^{-1}, recorded by the Wire 2.0 program supplied by Renishaw. With a high confocal mode (50× microscope objective), the vertical resolution is 3 to 4 μm, and the horizontal resolution is 1 μm.[36] Considering the relatively large size of the droplet, the signature of the surface region can be distinguished from that of the center region through the use of twice focus method, which is shown in Figure 1b.[36,37]

3. RESULTS AND DISCUSSION

3.1. LLPS of Mixed Droplets with OIR = 1:3 Deposited on a Hydrophobic Glass Slide. As reference systems, Raman spectra of a pure AS droplet, a pure phthalic acid droplet, and a mixed phthalic acid/AS droplet (OIR = 1:3) deposited on a hydrophobic glass slide coated with octadecanethiol are collected at approximately 293 K and ∼75% RH, as shown in Figure 2. The microscopy image of the mixed phthalic acid/AS droplet is given. The assignments of the peaks of phthalic acid, AS and H_2O, as listed in Table 1, are available in literature.[38−42]

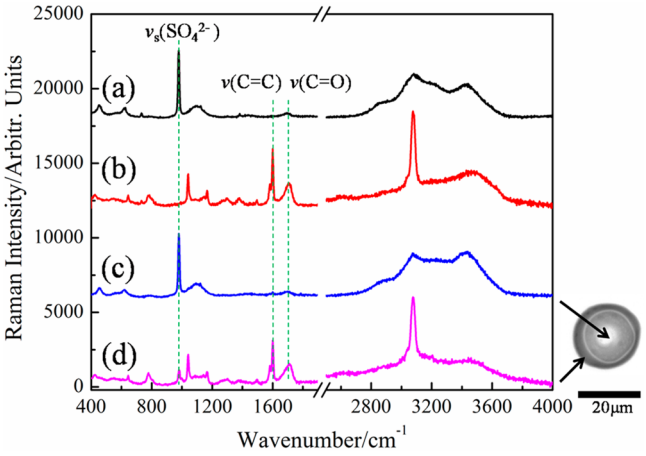

Figure 2. Raman spectra of (a) a pure AS droplet, (b) a pure phthalic acid droplet, (c) the inner phase, and (d) the outer phase of a mixed phthalic acid/AS droplet (OIR = 1:3) after phase separation on a hydrophobic glass slide. Length bar indicates 20 μm applied to the given particle image. All Raman spectra are collected at ∼293 K and ∼75% RH.

The morphology of the mixed droplet is an organic coating surrounding an aqueous AS core, with small amounts of each in the other phase. This is in line with the results reported by Ciobanu et al.; that is, the morphology of the particles with OIR = 1:2 to 1:8 is an aqueous AS inner core surrounded by the organic-rich outer phase.[15]

3.2. LLPS of Mixed Droplets with OIR = 1:3 on the PTFE-Coated Substrate. When the mixed phthalic acid/AS droplets are deposited on a quartz slide coated with a piece of hydrophobic PTFE film, the shape of droplets is nearly spherical, which has been introduced in the Experimental Section. In this case, the laser beam can be exactly focused twice at the surface and the center of the droplet, which provide special resolved Raman spectra from the surface and the center regions of the droplet. Figure 3 depicts the representative Raman spectra collected at the center and at the surface of the mixed droplet in the dehumidifying process. The RHs of LLPS and efflorescence of the mixed droplet are ∼75 and ∼50%, respectively, which are in line with the values reported in literature.[20]

The evolution of the physical state of the mixed droplet in dehumidifying process can be divided into three states: well-mixed liquid state, liquid−liquid phase-separated state, and crystalline state.

3.2.1. State I: Well-Mixed Liquid State at ∼90 to ∼80% RH. At ∼90% RH, the main features of spectra collected from the mixed phthalic acid/AS droplet show a sharp peak at ∼981 cm^{-1} and a weak peak at ∼1600 cm^{-1} as well as a rather weak peak at ∼1707 cm^{-1} (Figure 3), which correspond to the symmetric stretching mode of SO_4^{2-} and the stretching vibrations of C═C of benzene ring and C═O of carboxyl group of phthalic acid, respectively (Table 1). There is no difference for the Raman spectra collected at the center and at the surface, indicating that the mixed phthalic acid/AS droplet is homogeneous at ∼90% RH, as shown in Figure 4a.

When RH decreases to ∼80%, the diameter of the droplet shown in Figure 4b decreases in comparison with that shown in Figure 4a. The ν(C═C) peak at ∼1600 cm^{-1} and the ν(C═O) peak at ∼1707 cm^{-1} could be observed clearly at ∼80% RH from both Figure 3a,b, due to the increased of concentration of the droplet induced by the evaporation of water. However, there is no evident difference for the Raman spectra collected at the center and at the surface, which means that both AS and organics are still in a well-mixed liquid phase at this RH.

The difference values ΔR in the dehumidifying process are shown in Figure 5. It is obvious that at high RHs from ∼90 to ∼80% RH, the mixed droplet is in a well-mixed liquid phase, demonstrated by $\Delta R \approx 0$.

3.2.2. State II: Liquid−Liquid Phase-Separated State at ∼80 to ∼55% RH. In comparison with the dominance of the AS peak at ∼980 cm^{-1}, the spectral features of phthalic acid are hardly visible at the center region (Figure 3a), indicating that the inner phase is a highly concentrated aqueous AS solution containing small amounts of aqueous phthalic acid. At the same time, spectra acquired from the surface of the mixed droplet show well discernible signals of the aqueous phthalic acid bands, evidencing that the distribution of majority of aqueous phthalic acid is in the outer phase.

This phenomenon is further supported by the abruptly increase of ΔR in Figure 5 from ∼80 to ∼75% RH. The concentration of organics of the surface region is much higher than that of the center region, showing that the obvious phase-separation phenomenon occurs in the mixed droplet. Furthermore, ΔR is a positive value from ∼75 to ∼55% RH in Figure 5, and thus it can be concluded that the mixed droplet remains in a liquid−liquid phase-separated state.

Zuend et al. pointed out that LLPS into an organic-rich and an aqueous electrolyte phase can occur in the aerosols as a result of the salting-out effect.[43] On the basis of our results, we propose that the salting-out effect may induce the formation of the organic phase as well as the AS phase, thus leading to LLPS in the mixed droplets. The increase in ΔR at the RHs from ∼75 to ∼55% is an indicator of the diffusion of the organics from the inner phase to the outer phase. When RH decreased from ∼60

dx.doi.org/10.1021/jp5004598 | J. Phys. Chem. B 2014, 118, 6198−6205

Table 1. Molecular Vibration Assignments of Phthalic Acid/AS/Water System

	wavenumber in cm^{-1} and intensity[a,b]					
compound	(a)	(b)	(c)	(d)	ref	assignment[c]
ammonium sulfate $(NH_4)_2SO_4$	453 (w)		453 (w)	453 (w)	refs 41 and42	δ_s (SO_4^{2-})
	620 (w)		618 (w)	618 (w)		δ_{as}(SO_4^{2-})
	980 (vs)		981 (vs)	981 (w)		ν_s(SO_4^{2-})
	1102 (w)		1102 (w)			δ_{as}(SO_4^{2-})
phthalic acid $C_8H_6O_4$		643 (w)		643 (w)	refs 38−40	δ(OCO)
		780 (w)		780 (w)		r(OCO)
		1040 (vs)		1040 (vs)		δ(CH)
		1166 (m)		1166 (m)		ν(CH)
		1580(vs)		1580(vs)		ν(C═C)
		1600 (vs)		1600 (vs)		ν(C═C)
		1707 (vs)		1707 (vs)		ν(C═O)
		3077 (vs)		3077 (vs)		ν(CH)
water	3147 (m,b)	3255 (m,b)	3160 (m,b)	3248 (m,b)	ref 41	ν_s(OH)
	3422 (m,b)	3443 (m,b)	3427 (m,b)	3443 (m,b)		ν_{as}(OH)

[a](a) a pure AS droplet, (b) a pure phthalic acid droplet, (c) the core, and (d) the shell of a mixed phthalic acid/AS sulfate droplet after phase separation. [b]vs: very strong; s: strong; m: medium; w: weak; b: broad. [c]ν: stretching; δ: bending; r: rocking as antisymmetric mode; s: symmetric mode.

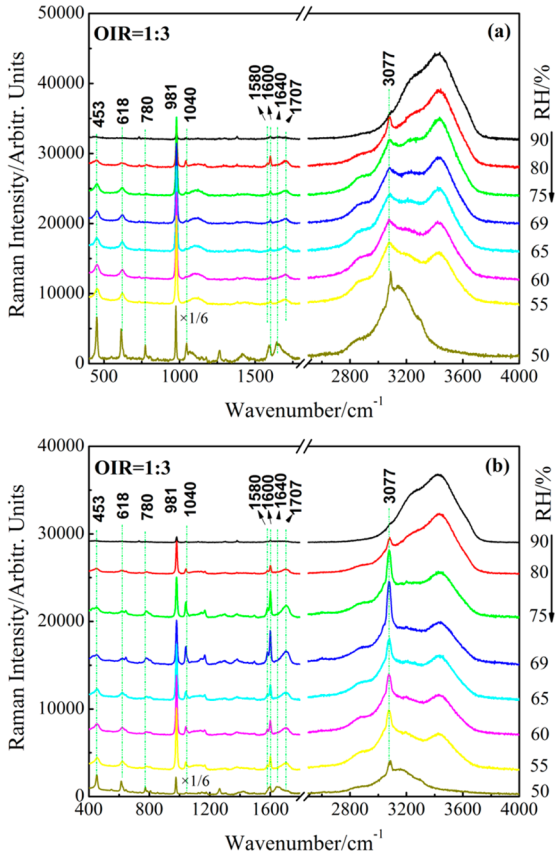

Figure 3. Raman spectra of the center (a) and the surface (b) of a mixed droplet (OIR = 1:3) on a PTFE substrate in the dehumidifying process. In both panels a and b, the peak heights of $\nu_s(SO_4^{2-})$ band located at ~981 cm^{-1} at ~50% RH are scaled by a factor of 1/6.

to ~55%, ΔR is decreased, as shown in Figure 5. As RH decreased from ~90 to ~55%, the radius of the droplet decreases by ~28 μm. At ~55% RH, which is close to the efflorescence RH (~50%), the droplet may be not spherical in shape, leading to the deviation of the measurements.

3.2.3. State III: Crystalline State at ~50% RH. When the RH decreases from ~90 to ~55%, the $\nu_s(SO_4^{2-})$ band of the center and surface regions has a red shift in peak position from 980.9 to 979.9 cm^{-1} and from 980.5 to 979.5 cm^{-1}, respectively. At ~50% RH, efflorescence of the droplet occurs. After efflorescence, the outer organic phase can no longer be distinguished from the inner AS phase by the micrograph (Figure 4f) or Raman spectra (Figure 3a,b). The efflorescence of AS is confirmed by the increased sharpness of the peaks at ~452 and ~618 cm^{-1} and the shift of the main peak position from ~980.9 to ~975.9 cm^{-1}, as shown in Figure 3. Such effects caused by the crystallization of AS have been described by Zhang and Chan.[44]

Furthermore, the ν(C═O) band of the center and surface regions of the mixed droplet has a red shift from ~1707 to ~1702 cm^{-1} and from ~1707 to ~1700 cm^{-1}, respectively, with the RH decreasing from ~90 to ~55%. The Raman spectra also provide clear evidence of the efflorescence of phthalic acid by the shift of the ν(C═O) band from ~1707 to ~1640 cm^{-1} as well as the emergence of a new peak at ~1590 cm^{-1}.

By using the scanning mode of Raman spectrometer, the relative spatial distribution of individual ingredients of the effloresced aerosol can be elucidated. For identification, the characteristic Raman peaks of AS (975 cm^{-1}) and phthalic acid (1040 cm^{-1}) are chosen as the peaks to be detected, as shown in Figure S2 of Supporting Information. In Figure S2a,b in the Supporting Information, the relative spatial distribution of AS and phthalic acid is in the center and in the edges of the effloresced aerosol (OIR = 1:3), respectively. The Raman micrograph of the phthalic acid/AS mixture again reveals the spatial separation of phthalic acid and AS in the effloresced aerosol in Figure S2c in the Supporting Information.

We also investigate LLPS in the mixed droplet with OIR = 1:6 in the dehumidifying process (see Figure S3, Supporting Information), and the evolution of the physical state (red dotted line in Figure 5) shows resemblance to that observed in the mixed droplet with OIR = 1:3.

3.3. Effect of Substrates and Possible Liquid−Liquid Phase-Separated Mechanism. To render the comparison of the effect of the substrates, we investigate mixed droplets on a hydrophilic glass slide. Raman spectra of a pure AS droplet, a pure phthalic acid droplet, and a mixed phthalic acid/AS

dx.doi.org/10.1021/jp5004598 | J. Phys. Chem. B 2014, 118, 6198−6205

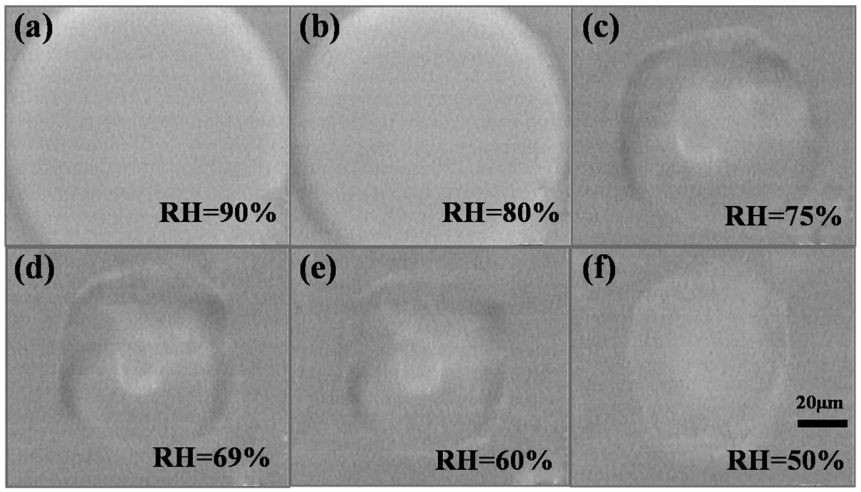

Figure 4. Raman micrographs of the mixed droplet (OIR = 1:3) on a PTFE substrate in the dehumidifying process. The length bar in the rightmost lower figure corresponds to 20 μm and applies to all six images.

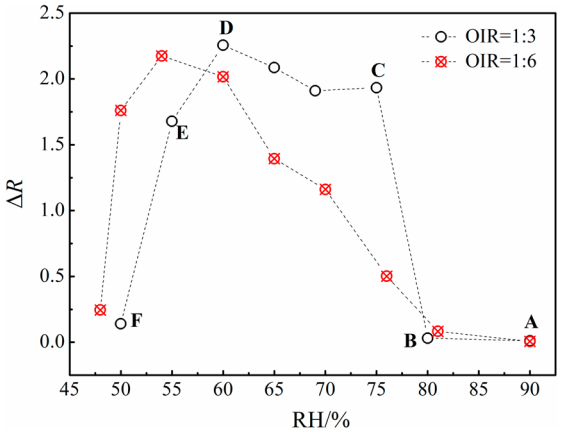

Figure 5. ΔR of the mixed droplet (with OIR = 1:3 and 1:6) as a function of RH in the dehumidifying process ($\Delta R = R_{center} - R_{surface}$, see the detailed information in the text).

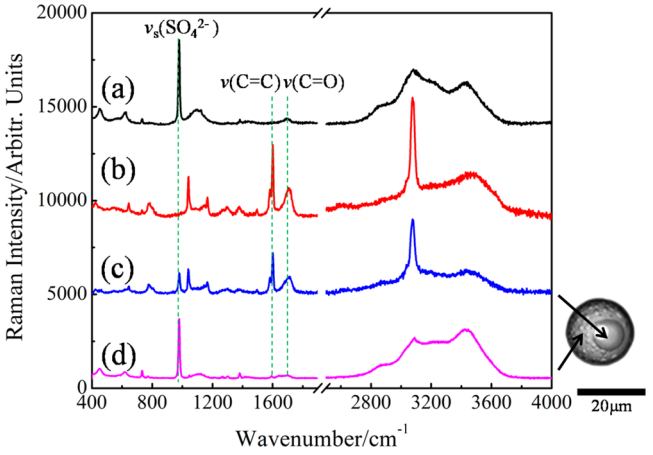

Figure 6. Raman spectra of (a) a pure AS droplet, (b) a pure phthalic acid droplet, (c) the inner phase, and (d) the outer phase of a mixed phthalic acid/AS droplet (OIR = 1:3) after phase separation on a hydrophilic glass slide. Length bar indicates 20 μm applying to the given particle image. All Raman spectra are collected at approximately 293 K and ~75% RH.

droplet (OIR = 1:3) deposited on a hydrophilic glass slide are collected at approximately 293 K and ~75% RH. As shown in Figure 6, the droplet on a hydrophilic glass slide is still in liquid–liquid phase-separated state, with the organic phase being the inner phase and the AS phase being the outer phase. The spatial distribution of an effloresced phthalic acid/AS aerosol (OIR = 1:3) on a hydrophilic glass slide is given in Figure S4 in the Supporting Information. The phenomenon is that phthalic acid has a high abundance in the center and AS mainly locates along the edges of the crystalline particle. The relative distributions of AS and phthalic acid observed by applying the scanning mode of Raman spectrometer are consistent with the previous results, while the relative spatial distribution of AS and phthalic acid is in the center and in the edges of the effloresced aerosol on the hydrophobic substrate, respectively, as shown in Figure S2 in the Supporting Information. It is interesting that the relative distribution of AS and organic phases of the mixed droplet on the hydrophilic substrate is contrary to that of the droplet on the hydrophobic substrate.

Liquid–liquid phase-separated mechanisms have received considerable attention and have been identified according to the morphologies developed at the onset of phase separation or during the growth of the second phase.[15] According to the results reported by Ciobanu et al.,[15] phase separation is observed to occur by fundamentally different mechanisms in dependence on OIR, namely, nucleation-and-growth (OIR = 8:1 to 2:1), spinodal decomposition (OIR = 1.5:1 to 1:1.5), and growth of a second phase at the surface of the particle (OIR = 1:2 to 1:8). The aerosol droplets in our experiments are with OIR = 1:3 and 1:6, which are in the range of OIR = 1:2 to 1:8 of the particles, therefore, we consider the growth of a second phase at the surface of the particle mechanism rather than nucleation-and-growth or the spinodal decomposition mechanism. Herein, combining the results about the evolution of the physical states and the comparison of the effect of substrates on the morphologies of droplets, the possible mechanisms that are responsible for the observed LLPSs on different substrates are proposed.

Figure 7 illustrates the effect of hydrophobic and hydrophilic substrates. At high RH, the mixed droplet is homogeneous. With the decrease in RH, the diffusion of the organics from the inner to the outer phase of the droplet occurs as a result of the salting-out effect, which induces the formation of the organic

dx.doi.org/10.1021/jp5004598 | J. Phys. Chem. B 2014, 118, 6198–6205

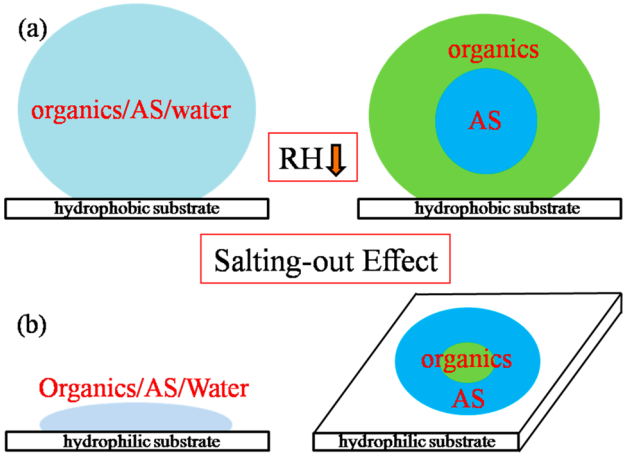

Figure 7. Schematic diagram for the effect of (a) hydrophobic and (b) hydrophilic substrates in the dehumidifying process. Left: well-mixed liquid state. Right: liquid–liquid phase-separated state. Brilliant blue, dark-blue, and green represent one aqueous phase, a liquid phase of AS, and a liquid phase of organic material, respectively.

phase as well as the AS phase. According to the results reported by Zuend et al., liquid–liquid phase equilibria in organic–inorganic systems are typically governed by strong interactions between electrically charged ions and nonpolar organic functional groups. Such organic–inorganic interactions may be the cause for LLPS due to salting-out effect.[15] For phthalic acid/AS droplets consisting of two liquid phases on the PTFE substrate, the outer phase was always the organic-rich phase, as shown in Figure 7a. From the consideration of surface tension, the equilibrium shape of a droplet containing two immiscible liquids will strive to assume a minimum surface energy. For liquids that are wetting each other, this is achieved when the liquid with lower surface tension is at the surface and uniformly covers the inner phase.[15] Phthalic acid has a lower surface tension (71.76 mN/m)[45] than aqueous AS solutions (88.80 mN/m).[46] Therefore, the outer and inner phases of the mixed droplets on a hydrophobic substrate are phthalic acid and AS, respectively. For the mixed droplets in which the surface tensions of the inorganic and organic compounds are quite different, the substrates are not the determining factor in the relative spatial distribution of the two phases. For instance, PEG-400 has a much lower surface tension (44.5 mN/m)[15] than AS solutions (88.8 mN/m),[46] and thus the resulting liquid–liquid phase-separated morphology of a mixed PEG-400/AS droplet is an aqueous AS inner phase surrounded by a mainly PEG-400 containing outer phase.[15] To prove that the substrates have no obvious effects on the distribution of these two phases in the droplets, we investigated a mixed PEG-400/AS droplet with OIR = 1:2 (the same OIR value as reported in ref 15) deposited on the hydrophilic substrate. As shown in Figure S5 in the Supporting Information, the Raman spectra of the outer phase and the inner phase of the droplet with LLPS at ~75% RH and the effloresced droplet at ~30% RH indicate that the relative distribution of PEG-400 and AS phases of the droplet on a hydrophilic substrate is the same as that of the droplets on a hydrophobic substrate.

It is noteworthy that when the surface tensions of the two compounds are close to each other the substrates may affect the relative distributions of the organic and inorganic phases of the mixed droplets. In our system, the surface tensions of phthalic acid and AS are 71.76 and 88.80 mN/m, respectively. Different from the condition that AS inner phase of the droplets deposited on the hydrophobic substrate is surrounded by phthalic acid outer phase, the organics is the inner phase when the mixed droplet is dropped on the hydrophilic substrate, as shown in Figure 7b. In this case, the relative distributions of the two phases in the droplets can be mainly affected by the substrates.

In Figure 7b, a plane graph of the mixed droplet on the hydrophilic substrate is shown. The aqueous AS may be attracted by the hydrophilic surface, and thus the lower density organic phase may float on top in the center of the inorganic flat layer. Because the thickness of the droplet is out of the vertical resolution of the confocal Raman spectrometer, it is hard to make sure the exact position of the organic phase in the vertical direction of the droplet. However, we can still draw the confirm conclusions about the relative spatial distribution in the horizontal direction by applying Raman spectroscopy.

On the basis of the literature data,[47] several possible sites where crystal nucleation can occur for a droplet deposited on a substrate have been reported: (1) at the droplet/substrate interface (efflorescence relative humidity (ERH) > 40%), (2) at the air/droplet interface (in the range from 36 to 40% RH), (3) along the air/droplet/substrate contact line (in the range from 36 to 40% RH), and (4) in the volume of the droplet (ERH < 34%). In our systems, ERHs are ~50%; therefore, the possible sites where AS nucleation occurs may be at the droplet/substrate interface. Takahama et al.[48] found the existence of layered morphologies (organic outer phase around inorganic inner phase) of ambient particles collected onto a hydrophobic substrate (silicon nitride) by X-ray microscopy and provided useful methods for visualizing the sphericity of the particle and calculating the shell thickness. The vertical structures of phthalic acid/AS mixed droplets with LLPS deposited on the hydrophilic substrate may be explored in the future experiments by applying this method.

The different spatial distributions of AS and phthalic acid in the mixed aerosol droplets are attributed to the surface tensions of phthalic acid and AS phases and the effect of hydrophobic and hydrophilic substrates. The surface tension of organic phase is invariably smaller than that of inorganic phase, which induces the outer phases of the mixed droplets deposited on hydrophobic substrates to be mostly the organic-rich phase. When the values of the surface tension of organic and inorganic compounds are close to each other, the relative distribution of the two phases in the mixed droplets may be affected by the substrates.

In summary, we elucidate the evolution of the physical state of mixed droplets in the dehumidifying process by describing the differences of compositions between the center and the surface regions of the mixed droplet. Three states can be found, that is, well-mixed liquid state, liquid–liquid phase-separated state, and crystalline state. In addition, the surface tension and hydrophobicity/hydrophilicity of substrates influence the spatial distribution of phthalic acid and AS in mixed aerosols with liquid–liquid phase-separated state.

4. CONCLUSIONS

We have shown the evolution of the physical state of mixed phthalic acid/AS droplets (OIR = 1:3 and 1:6) deposited on a PTFE substrate by using confocal Raman technology combined with optical microscopy. The evolution of the physical state of the mixed droplet in the dehumidifying process consists of three states, that is, well-mixed liquid state, liquid–liquid phase-

dx.doi.org/10.1021/jp5004598 | J. Phys. Chem. B 2014, 118, 6198–6205

separated state, and crystalline state. We propose that the salting-out effect may induce the formation of the organics phase as well as the AS phase, thus leading to LLPS in aerosol droplets. Both the surface tension and hydrophobicity/hydrophilicity of substrates influence the spatial distribution of a mixed phthalic acid/AS aerosol with two liquid phases. The surface tension of organic phase is invariably smaller than that of inorganic phase. When the values of the surface tension of organic and inorganic compounds are close to each other, the relative distribution of the two phases in the mixed droplets may be affected by the substrates, while when the values of the surface tension of organic and inorganic compounds differ considerably, the surface tension is the main factor for the relative distribution of the two phases in the mixed droplets.

The understanding about the evolution of the physical state of mixed phthalic acid/AS droplets may shed light on the formation of atmospheric aerosols' morphology in the dehumidifying process and provides necessary information to the investigations of the kinetics of tropospheric aerosols.

■ ASSOCIATED CONTENT

Supporting Information

Information about the relative spatial distribution of the two liquid phases of mixed aerosols dropped on a hydrophobic glass slide and a hydrophilic glass slide. This material is available free of charge via the Internet at http://pubs.acs.org.

■ AUTHOR INFORMATION

Corresponding Authors

*J.-B.M.: Tel: 86-10-68913596. E-mail: majiabi@bit.edu.cn.
*Y.-H.Z.: E-mail: yhz@bit.edu.cn.

Notes

The authors declare no competing financial interest.

■ ACKNOWLEDGMENTS

We gratefully appreciate financial support from the National Natural Science Foundation of China (41175119 and 20933001), the 111 Project (B07012), and Beijing Natural Science Foundation (2144055). We wish to express our gratitude to the anonymous reviewers for the stimulating suggestions and discussions.

■ REFERENCES

(1) Buzorius, G.; Zelenyuk, A.; Brechtel, F.; Imre, D. Simultaneous Determination of Individual Ambient Particle Size, Hygroscopicity and Composition. *Geophys. Res. Lett.* **2002**, *29*, 35.
(2) Pratt, K. A.; Prather, K. A. Aircraft Measurements of Vertical Profiles of Aerosol Mixing States. *J. Geophys. Res.* **2010**, *115*, D11305.
(3) Huebert, B. J.; Howell, S. G.; Zhuang, L.; Heath, J. A.; Litchy, M. R.; Wylie, D. J.; Kreidler-Moss, J. L.; Coppicus, S.; Pfeiffer, J. E. Filter and Impactor Measurements of Anions and Cations During the First Aerosol Characterization Experiment (ACE 1). *J. Geophys. Res.* **1998**, *103*, 16493−16509.
(4) Talbot, R. W.; Dibb, J. E.; Loomis, M. B. Influence of Vertical Transport on Free Tropospheric Aerosols over the Central USA in Springtime. *Geophys. Res. Lett.* **1998**, *25*, 1367−1370.
(5) Jacobson, M. C.; Hansson, H. C.; Noone, K. J.; Charlson, R. J. Organic Atmospheric Aerosols: Review and State of the Science. *Rev. Geophys.* **2000**, *38*, 267−294.
(6) Gouw, J. D.; Jimenez, J. Organic Aerosols in the Earth's Atmosphere. *Environ. Sci. Technol.* **2009**, *43*, 7614−7618.
(7) Tost, H.; Pringle, K. J. Improvements of Organic Aerosol Representations and Their Effects in Large-Scale Atmospheric Models. *Atmos. Chem. Phys.* **2012**, *12*, 8687−8709.
(8) Hansen, J.; Sato, M.; Ruedy, R.; Lacis, A.; Oinas, V. Global Warming in the Twenty-first Century: An Alternative Scenario. *Proc. Natl. Acad. Sci. U. S. A.* **2000**, *97*, 9875−9880.
(9) Lelieveld, J.; Heintzenberg, J. Sulfate Cooling Effect on Climate Through In-Cloud Oxidation of Anthropogenic SO_2. *Science* **1992**, *258*, 117−120.
(10) Wang, L.; Xu, W.; Khalizov, A. F.; Zheng, J.; Qiu, C.; Zhang, R. Y. Heterogeneous Reactions of Epoxides in Acidic Media. *J. Phys. Chem. A* **2011**, *115*, 8940−8947.
(11) Decesari, S.; Fuzzi, S.; Facchini, M. C.; Mircea, M.; Emblico, L.; Cavalli, F.; Maenhaut, W.; Chi, X.; Schkolnik, G.; Falkovich, A.; et al. Characterization of the Organic Composition of Aerosols from Rondonia, Brazil, during the LBA-SMOCC 2002 Experiment and Its Representation through Model Compounds. *Atmos. Chem. Phys.* **2006**, *6*, 375−402.
(12) Goldstein, A. H.; Galbally, I. E. Known and Unexplored Organic Constituents in the Earth's Atmosphere. *Environ. Sci. Technol.* **2007**, *41*, 1514−1521.
(13) Turpin, B. J.; Saxena, P.; Andrews, E. Measuring and Simulating Particulate Organics in the Atmosphere: Problems and Prospects. *Atmos. Environ.* **2000**, *34*, 2983−3013.
(14) Hallquist, M.; Wenger, J. C.; Baltensperger, U.; Rudich, Y.; Simpson, D.; Claeys, M.; Dommen, J.; Donahue, N. M.; George, C.; Goldstein, A. H.; et al. The Formation, Properties and Impact of Secondary Organic Aerosol: Current and Emerging Issues. *Atmos. Chem. Phys.* **2009**, *9*, 5155−5236.
(15) Ciobanu, V. G.; Marcolli, C.; Krieger, U. K.; Weers, U.; Peter, T. Liquid−Liquid Phase Separation in Mixed Organic/Inorganic Aerosol Particles. *J. Phys. Chem. A* **2009**, *113*, 10966−10978.
(16) Kwamena, N. O. A.; Buajarern, J.; Reid, J. P. Equilibrium Morphology of Mixed Organic/Inorganic/Aqueous Aerosol Droplets: Investigating the Effect of Relative Humidity and Surfactants. *J. Phys. Chem. A* **2010**, *114*, 5787−5795.
(17) Reid, J. P.; Dennis-Smither, B. J.; Kwamena, N. O. A.; Miles, R. E. H.; Hanford, K. L.; Homer, C. J. The Morphology of Aerosol Particles Consisting of Hydrophobic and Hydrophilic Phases: Hydrocarbons, Alcohols and Fatty Acids as the Hydrophobic Component. *Phys. Chem. Chem. Phys.* **2011**, *13*, 15559−15572.
(18) Dennis-Smither, B. J.; Hanford, K. L.; Kwamena, N. O. A.; Miles, R. E. H.; Reid, J. P. Phase, Morphology, and Hygroscopicity of Mixed Oleic Acid/Sodium Chloride/Water Aerosol Particles before and after Ozonolysis. *J. Phys. Chem. A* **2012**, *116*, 6159−6168.
(19) Krieger, U. K.; Marcolli, C.; Reid, J. P. Exploring the Complexity of Aerosol Particle Properties and Processes Using Single Particle Techniques. *Chem. Soc. Rev.* **2012**, *41*, 6631−6662.
(20) Song, M.; Marcolli, C.; Krieger, U. K.; Lienhard, D. M.; Peter, T. Morphologies of Mixed Organic/Inorganic/ Aqueous Aerosol Droplets. *Faraday Discuss.* **2013**, *165*, 289−316.
(21) Bertram, A. K.; Martin, S. T.; Hanna, S. J.; Smith, M. L.; Bodsworth, A.; Chen, Q.; Kuwata, M.; Liu, A.; You, Y.; Zorn, S. R. Predicting the Relative Humidities of Liquid−Liquid Phase Separation, Efflorescence, and Deliquescence of Mixed Particles of Ammonium Sulfate, Organic Material, and Water Using the Organic-to-Sulfate Mass Ratio of the Particle and the Oxygen-to-Carbon Elemental Ratio of the Organic Component. *Atmos. Chem. Phys.* **2011**, *11*, 10995−11006.
(22) You, Y.; Renbaum-Wolff, L.; Bertram, A. K. Liquid−liquid Phase Separation in Particles Containing Organics Mixed with Ammonium Sulfate, Ammonium Bisulfate, Ammonium Nitrate or Sodium Chloride. *Atmos. Chem. Phys.* **2013**, *13*, 11723−11734.
(23) Song, M.; Marcolli, C.; Krieger, U. K.; Zuend, A.; Peter, T. Liquid-Liquid Phase Separation and Morphology of Internally Mixed Dicarboxylic Acids/Ammonium Sulfate/Water Particles. *Atmos. Chem. Phys.* **2012**, *12*, 2691−2712.
(24) Vazquez, G. J.; Dodge, C. J.; Francis, A. J. Interaction of Uranium(VI) with Phthalic Acid. *Inorg. Chem.* **2008**, *47*, 10739−10743.
(25) Pavuluri, C. M.; Kawamura, K. New Directions: Need for Better Understanding of Plastic Waste Burning as Inferred from High

Abundance of Terephthalic Acid in South Asian Aerosols. *Atoms. Environ.* **2010**, *44*, 5320−5321.
(26) Wang, G. H.; Kawamura, K.; Cheng, C. L.; Li, J. J.; Cao, J. J.; Zhang, R. J.; Zhang, T.; Liu, S. X.; Zhao, Z. Z. Molecular Distribution and Stable Carbon Isotopic Composition of Dicarboxylic Acids, Ketocarboxylic Acids, and α-Dicarbonyls in Size-Resolved Atmospheric Particles From Xi'an City, China. *Environ. Sci. Technol.* **2012**, *46*, 4783−4791.
(27) Martin, S. T. Phase Transitions of Aqueous Atmospheric Particles. *Chem. Rev.* **2000**, *100*, 3403−3453.
(28) Colberg, C. A.; Luo, B. P.; Wernli, H.; Koop, T.; Peter, T. A Novel Model to Predict the Physical State of Atmospheric H_2SO_4/NH_3/H_2O Aerosol Particles. *Atmos. Chem. Phys.* **2003**, *3*, 909−924.
(29) Ling, T. Y.; Chan, C. K. Partial Crystallization and Deliquescence of Particles Containing Ammonium Sulfate and Dicarboxylic Acids. *J. Geophys. Res.* **2008**, *113*, D14205.
(30) Yeung, M. C.; Lee, A. K. Y.; Chan, C. K. Phase Transition and Hygroscopic Properties of Internally Mixed Ammonium Sulfate and Adipic Acid (AS-AA) Particles by Optical Microscopic Imaging and Raman Spectroscopy. *Aerosol Sci. Technol.* **2009**, *43*, 387−399.
(31) Miñambres, L.; Sánchez, M. N.; Castaño, F.; Basterretxea, F. J. Hygroscopic Properties of Internally Mixed Particles of Ammonium Sulfate and Succinic Acid Studied by Infrared Spectroscopy. *J. Phys. Chem. A* **2010**, *114*, 6124−6130.
(32) Han, N. Y.; Zhu, L.; Wang, L. S.; Fu, R. N. Aqueous Solubility of m-Phthalic Acid, o-Phthalic Acid and p-Phthalic Acid from 298 to 483 K. *Sep. Purif. Technol.* **1999**, *16*, 175−180.
(33) Parsons, M. T.; Knopf, D. A.; Bertram, A. K. Deliquescence and Crystallization of Ammonium Sulfate Particles Internally Mixed with Water-Soluble Organic Compounds. *J. Phys. Chem. A* **2004**, *108*, 11600−11608.
(34) Park, B. H.; Lee, M. H.; Kim, S. B.; Jo, Y. M. Evaluation of the Surface Properties of PTFE Foam Coating Filter Media Using XPS and Contact Angle Measurements. *Appl. Surf. Sci.* **2011**, *257*, 3709−3716.
(35) Khismatullin, D. B.; Nadim, A. Shape Oscillations of A Viscoelastic Drop. *Phys. Rev. E* **2001**, *63*, 061508.
(36) Li, K. K.; Wang, F.; Zeng, G.; Reid, J. P.; Zhang, Y. H. Probing the Time Scale for Bulk Equilibration and Mass Transport of Water in Amorphous Inorganic Aerosol. *J. Phys. Chem. B* **2011**, *115*, 14397−14403.
(37) Yu, J. Y.; Zhang, Y.; Zeng, G.; Zheng, C. M.; Liu, Y.; Zhang, Y. H. Suppression of $NaNO_3$ Crystal Nucleation by Glycerol: Micro-Raman Observation on the Efflorescence Process of Mixed Glycerol/$NaNO_3$/Water Droplets. *J. Phys. Chem. B* **2012**, *116*, 1642−1650.
(38) Osterrothová, K.; Jehlicka, J. Raman Spectroscopic Identification of Phthalic and Mellitic Acids in Mineral Matrices. *Spectrochim. Acta, Part A* **2010**, *77*, 1092−1098.
(39) Osterrothová, K.; Jehlicka, J. Feasibility of Raman Microspectroscopic Identification of Biomarkers through Gypsum Crystals. *Spectrochim. Acta, Part A* **2011**, *80*, 96−101.
(40) Klug, O.; Parlagh, G.; Forsling, W. Raman Spectroscopy of Aromatic Acids Adsorbed on Oxidised Aluminium Foil. *J. Mol. Struct.* **1997**, *410*−*411*, 183−188.
(41) Dong, J. L.; Li, X. H.; Zhao, L. J.; Xiao, H. S.; Wang, F.; Guo, X.; Zhang, Y. H. Raman Observation of the Interactions between NH_4^+, SO_4^{2-}, and H_2O in Supersaturated $(NH_4)_2SO_4$ Droplets. *J. Phys. Chem. B* **2007**, *111*, 12170−12176.
(42) Colberg, C. A. *Experimente an Levitierten H_2SO_4/NH_3/H_2O-Aerosolteilchen: Atmospharische Relevanz von Letovizit*. Ph.D. Dissertation, ETH Zurich, 2001; no. 14331.
(43) Zuend, A.; Marcolli, C.; Peter, T.; Seinfeld, J. H. Computation of Liquid−Liquid Equilibria and Phase Stabilities: Implications for RH Dependent Gas/Particle Partitioning of Organic−Inorganic Aerosols. *Atmos. Chem. Phys.* **2010**, *10*, 7795−7820.
(44) Zhang, Y. H.; Chan, C. K. Understanding the Hygroscopic Properties of Supersaturated Droplets of Metal and Ammonium Sulfate Solutions Using Raman Spectroscopy. *J. Phys. Chem. A* **2002**, *106*, 285−292.
(45) Padro, L. T.; Nenes, A. Cloud Droplet Activation: Solubility Revisited. *Atmos. Chem. Phys. Discuss.* **2007**, *7*, 2325−2355.
(46) Lewis, E. R. The Effect of Surface Tension (Kelvin Effect) on the Equilibrium Radius of a Hygroscopic Aqueous Aerosol Particle. *J. Aerosol Sci.* **2006**, *37*, 1605−1617.
(47) Ciobanu, V. G.; Marcolli, C.; Krieger, U. K.; Zuend, A.; Peter, T. Efflorescence of Ammonium Sulfate and Coated Ammonium Sulfate Particles: Evidence for Surface Nucleation. *J. Phys. Chem. A* **2010**, *114*, 9486−9495.
(48) Takahama, S.; Liu, S.; Russell, L. M. Coatings and Clusters of Carboxylic Acids in Carbon-containing Atmospheric Particles from Spectromicroscopy and Their Implications for Cloud-Nucleating and Optical Properties. *J. Geophys. Res.* **2010**, *115*, D01202.